Available online at www.eccomasproceedia.org
Eccomas Proceedia COMPDYN (2021) 5165-5178

ECCOMAS
Proceedia

COMPDYN 2021
8th ECCOMAS Thematic Conference on
Computational Methods in Structural Dynamics and Earthquake Engineering
M. Papadrakakis, M. Fragiadakis (eds.)
Streamed from Athens, Greece, 28 - 30 June 2021

PARAMETRIC STUDY OF STEEL COLUMN-BASE CONNECTION SUBJECTED TO BIDIRECTIONAL BENDING AND AXIAL COMPRESSION

Md. Asif B. Kabir[1], and AHM M. Billah[2]

[1] Graduate Research Assistant
Lakehead University, Thunder Bay, ON, Canada
e-mail: mkabir4@lakeheadu.ca

[2] Assistant Professor
Lakehead University, Thunder Bay, ON, Canada
e-mail: muntasir.billah@lakeheadu.ca

Abstract

Column base plate connection is one of the most critical structural components of steel moment-resisting frames which acts as a transfer medium to transmit the reaction forces, shear and moments from the entire building into the foundation. Failure of these base plate connections is critical since it can result in the collapse of the entire structure. Very often these base plates experience bidirectional lateral loadings from natural events such as wind and earthquake. Previous studies considered uniaxial lateral loading combined with axial load but do not provide any guidelines for exposed column base plate connections under axial load and biaxial lateral loading. This study aims to develop an accurate nonlinear finite element (FE) model of exposed column-base connections under combined axial load and bi-axial lateral loading using general purpose finite element software ABAQUS. The developed model is validated against experimental results under monotonic and cyclic loading considering both geometric and material nonlinearities to check the accuracy of the model. After validation, a bidirectional symmetric lateral loading combined with constant axial compressive load is applied in the developed model to analyze the response of the column-base plate connections. Further, the effects of three different parameters of column base plate connection such as base plate thickness, base plate yield strength, and anchor rod diameter are investigated through parametric study. Results show that higher value of base plate thickness and anchor rod diameter significantly affect both the stiffness and strength of column base connections. It also demonstrates that base plate yield strength has no significant influence on column base connections.

Keywords: Column Base Plate Connection, Bidirectional Lateral Loading, Finite Element Modeling, Parametric Study.

ISSN:2623-3347
Peer-review under responsibility of the organizing committee of COMPDYN 2021.
doi: 10.7712/120121.8857.19561

1 INTRODUCTION

In steel moment-resisting frames, column base plate (CBP) connection is one of the most critical structural components that transfer the forces and moments from the superstructure to the substructure. Under dynamic loadings, such as earthquake and wind, the dynamic effects are transferred to the structure through the base plate of this connection. Failure of the CBP connection can result in the collapse of the entire frame as the ductility demand and force distribution in the structure is directly affected [1]. Tremblay et al. [2] and Midorikawa et al. [3] outlined several issues with the exposed type CBP connections experienced during the past major seismic events (e.g. 2011 Tohuku, 1995 Kobe, 1994 Northridge). Exposed column base connections are mostly found in low-rise steel structures around the world. Over the past forty years, researchers have extensively investigated various parameters, both experimentally and numerically, affecting the design, behavior, and strength of CBP connections [4-7]. These research outcomes led to the publication of the AISC Design Guide 1 [8] for column base plate design, which is still widely used in the industry. Fahmy et al. [9] examined the base connection failure mechanisms and categorized them into three main groups as "weak column-strong connection", "balanced mechanism", and "strong column-weak connection". All of these previous studies and design guidelines focused on the base plate design under axial load and uniaxial bending moment although the base plates very often can experience bidirectional bending moment from lateral loads. Though the columns are designed and checked considering axial load and biaxial bending, when it comes to the base plate connection, only the axial load combined with major axis bending is considered.

Lee et al. [10, 11] experimentally and numerically investigated the response of CBP connections under weak axis moments. They concluded that the widely used Drake and Elkin's design method is inadequate for designing CBP connections under minor axis bending. Gomez et al. [12] formulated a new technique for characterizing the strength of the CBP connections by introducing a plastic mechanism through extensive experimental study. This study was further expanded by Kanvinde et al. [13] through finite element (FE) analysis to investigate the stress distribution in different components of CBP connections. Although very effective, both of them concluded that the recommended method is not applicable for designing CBP connections under biaxial bending. Fasaee et al. [14] conducted a numerical investigation to evaluate the capacity of flexible CBP connections under axial load and biaxial bending. They proposed an analytical model to determine the moment capacity along the major and minor axis considering the variation of applied axial load only. Recently, Song et al. [15] performed a reliability analysis of CBP connections under combined axial compression and flexure. They identified AISC Design Guide 1 [8] approach to be inconsistent which underestimated the flexural demand in the base plate and inapplicable for CBP connections under biaxial bending. Although they proposed two alternative design approaches for overcoming these limitations and improving the reliability, however, those are only applicable under uniaxial bending.

Currently, there exists a gap in the literature that comprehensively investigates the behavior of exposed CBP connections subjected to combined axial load and biaxial bending. Hence, this study aims to investigate the behavior of the W-shaped steel CBP connection under combined axial load and biaxial bending through parametric numerical analysis. This is achieved through the pursuit of considering different values for three parameters of CBP connections such as base plate thickness, base plate yield strength, and anchor rod diameter.

2 FINITE ELEMENT MODELING – METHODOLOGY AND VALIDATION

A detailed 3D nonlinear finite element (FE) model is developed using ABAQUS [16] simulation platform. FE model constructed for validation in this study considered the geometric

and material properties of CBP connections experimented by Gomez et al. [12]. The FE model is developed and validated in two phases where the model is constructed as a half model first due to the symmetric nature of the specimen under monotonic loading to reduce the simulation time for interpreting a suitable modeling strategy. Later, a full FE model is developed instead of the half-model to simulate the accurate behavior under combined axial load and lateral cyclic loading. A description of the overall methodology to develop the FE model followed by the validation of the developed models is presented in the subsequent sections.

2.1 Methodology

All the elements are modelled as 3D deformable solid elements except the column in the full model which is defined as shell elements for validating the complex cyclic simulation with the consideration of global and local buckling behavior [17]. The column is considered as a W200x71 section which reflects the typical members that are used as the first-story interior columns of steel moment resisting frames (SMRF). The length of the column is considered as 2350 mm from the top of the base plate. The cross-sectional dimension of the grout is considered the same as the base plate dimension (356mm x 356mm). A 1220x1220x610 mm concrete footing is considered for the foundation of the CBP connection. Figure 1 shows details of the geometry and dimensions of the specimens used to validate the FE model.

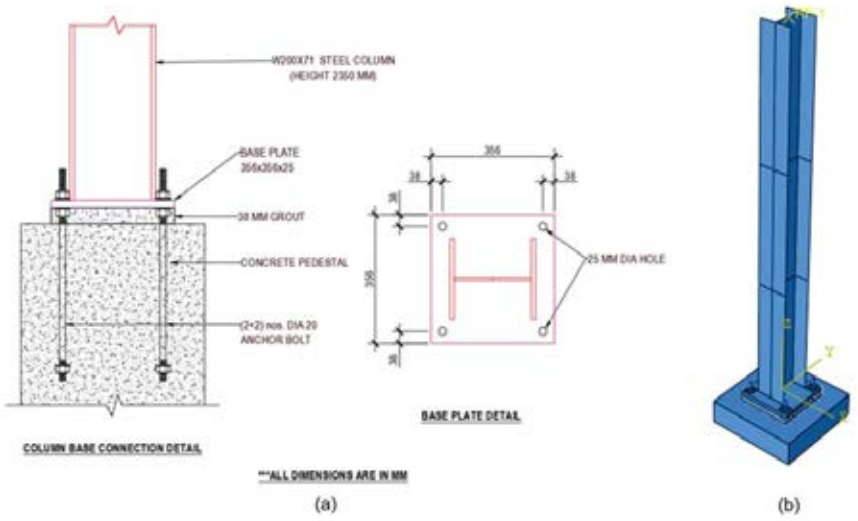

Figure 1: (a) Geometric details (b) Developed FE model

All the 3D solid elements of the developed model are meshed with hexahedral (C3D8R) element whereas the shell element of the column is meshed with quadratic 4-node doubly curved (S4R) shell elements accumulating a total number of 82000 elements. Geometric nonlinearity (NLGEOM) is considered due to the nonlinear effects of large displacement. Column is meshed by dividing its length into three equal parts for computational efficiency. The bottom part is meshed using the same element size as the base plate to neglect the convergence issue while the other parts are meshed using a coarser mesh size. Grout is also meshed by a size similar to the column bottom part and base plate. Anchor rods, nuts and washer are meshed using finer element size to accurately capture the stress behavior of these elements. Since the behavior of footing is not considered in this study, larger mesh size is considered for the footing. A mesh sensitivity study is conducted to accurately predict the results as well as to ensure the computational time efficiency of the developed FE models. For brevity, the details

of the mesh sensitivity study are omitted from this paper. It is very usual for steel structural elements to contain geometric imperfections as well as residual stresses due to the manufacturing and handling process. Geometric imperfection is introduced to capture the global out-of-straightness imperfections of the column. Separate linear perturbation buckling analysis is performed to obtain different buckling modes of the respective column. A global out-of-straightness limit equal to L/1500 [17] is applied with the first buckling mode of the column during the construction of the full model under cyclic loading.

Explicit modeling of component interaction is critical as the contact and gapping of CBP connection components control the overall connection response [13]. Tie constraints are provided between the column and base plate, anchor rods, nuts, and washers, and between the grout and concrete because of their monolithic properties. Surface to surface contact interactions are defined between the interfaces of the base plate and grout, base plate and both the top and bottom washer, and anchor rod-base plate with the finite sliding formulation. Two different interaction properties are defined for these surface to surface interactions. A coefficient of friction of 0.45 is used for the base plate and grout whereas 0.80 is used for the other two interactions [18]. The pressure overclosure for normal behavior is considered as hard contact and separation after contact is allowed whereas the constraint enforcement method is set as default for both the interaction properties. No constraints or interactions are defined between the concrete footing and the anchor rods assuming their interfaces to be free as prescribed by Gomez et al. [12]. Figure 2 illustrates a schematic description of contact and interactions between different components of CBP connection.

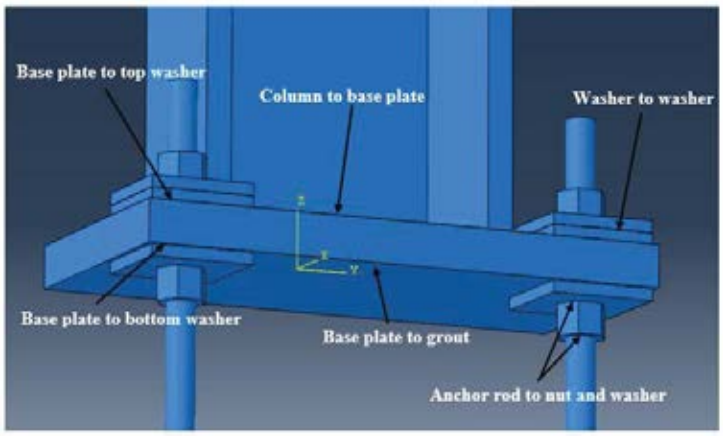

Figure 2: Contact and interactions of different components of CBP connection

The bottom of the concrete footing is restrained in all six degrees of freedom to simulate a fixed-base condition. When the FE model is constructed as a half model under monotonic loading, a symmetric boundary condition is provided parallel to the center plane of the column web to simulate its full-scale behavior. On the other hand, to accurately capture the flexural yielding and geometric instabilities under cyclic loading with full model, a flexible boundary condition is considered at a reference point defined at the cross-section center of the top of the column.

2.2 Material modeling

Steel Elements: Von-Mises type of material with a nonlinear isotropic/kinematic hardening material model is used to define the column and base plate. In addition to the modulus of elasticity and yield stress, the nonlinear kinematic and isotropic hardening components (C, γ, Q_∞, b) are considered for cyclic loading which are derived from the Chaboche [19] model. A

nonlinear monotonic isotropic hardening is modeled for anchor rod whereas nut and washer are modeled as elastic-perfectly plastic material. The hardening parameters used for these parts are from the results of the ancillary experiments conducted by Gomez et al. [12]. Table 1 and 2 provides the values used to define different steel materials for validation of developed FE model for monotonic and cyclic loadings, respectively.

	Yield Stress (MPa)	Modulus of Elasticity (GPa)	Poisson's ratio	Material type
Column	345	200	0.3	nonlinear isotropic hardening
Base Plate	280	200	0.3	nonlinear isotropic hardening
Anchor Rod	786	200	0.3	nonlinear isotropic hardening
Nut & Washer	345	200	0.3	elastic perfectly plastic

Table 1: Steel material for monotonic loading

	Yield Stress (MPa)	Modulus of Elasticity (GPa)	Poisson's ratio	C (MPa)	γ	Q∞ (MPa)	b
Column	380	200	0.3	3378	20	90	12
Base Plate	255	216	0.3	6895	25	172	2
Anchor Rod	790	200	0.3	nonlinear isotropic hardening			
Nut & Washer	345	200	0.3	elastic perfectly plastic			

Table 2: Steel material for cyclic loading

Concrete Elements: Concrete damage plasticity model is developed based on compressive strength for both grout and concrete pedestal. The compressive strengths used for developing concrete damage plasticity model are adopted from the ancillary test results by Gomez et al. [12] for both footing & grout. For monotonic loading phase, the compressive strength of grout and footing is considered as 51 and 27 MPa, respectively. Similarly, the compressive strength of grout and footing is considered as 64 and 30 MPa, respectively for the cyclic loading case. Default values were used for the other parameters to define the concrete damage plasticity model as provided in Table 3.

Parameters	Value
Dilation angle (ψ)	36^0
Eccentricity (e)	0.1
fb_o/fc_o	1.16
K	0.6667
Viscosity parameter	0.001

Table 3: Concrete damage plasticity parameters

2.3 Loading protocol

At first, monotonic loading in the form of lateral displacement (10.58% column drift) is applied along the major axis direction with no axial load. After validating under monotonic load, SAC cyclic loading protocol with a maximum drift of 10.6% is applied in the column major axis direction with a constant 410 KN axial compression at the top of the column to validate the model accuracy under combined axial load and uniaxial cyclic loading.

2.4 Validation of developed FE model

The developed FE model is validated against experimental results from Gomez et al. [12] under monotonic and cyclic loading for Test no. 1 and Test no. 5, respectively to check the accuracy of the adopted modeling approach. For monotonic loading, the developed half FE model is validated in terms of anchor rod force and base plate deformation profile as shown in Figure 3 and 4, respectively. From both the Figures, it can be seen that the developed FE model can very well predict the experimental results with reasonable accuracy signifying the suitability of the adopted modeling techniques and material models.

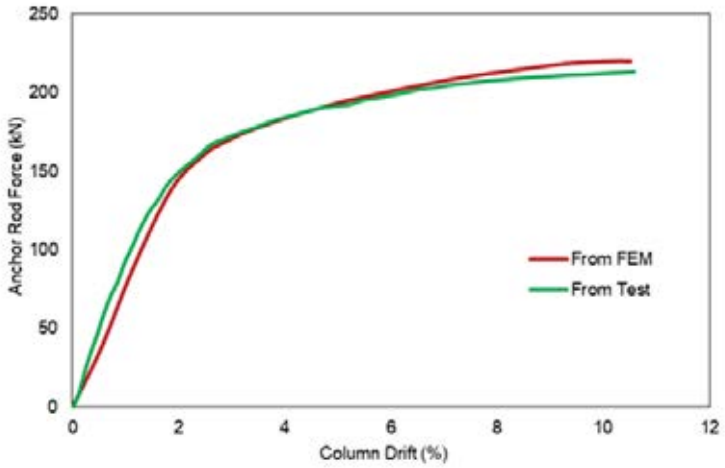

Figure 3: Comparison of experimental (Gomez et al. [12] Test no. 1) and numerical (FE) results

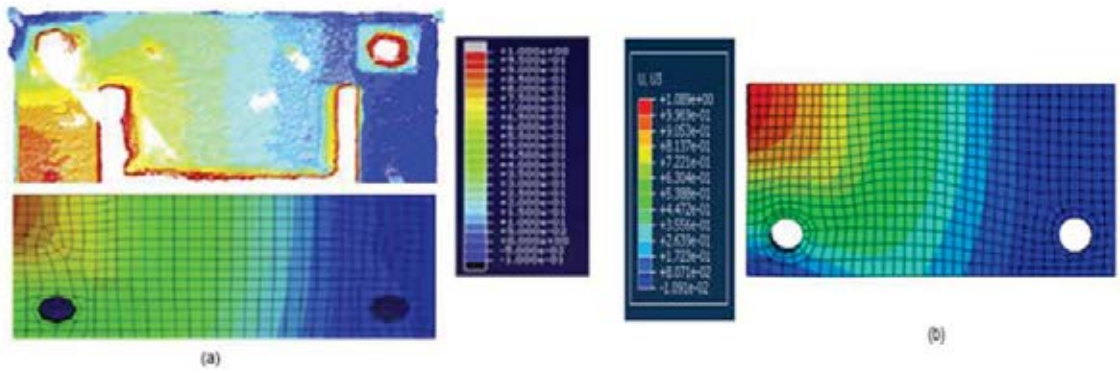

Figure 4: Base plate deformation behavior (a) Gomez et al. [12] Test no.1 (b) developed FE model

Further, the full FE model is validated under cyclic loading protocol in terms of the lateral load-displacement profile as shown in Figure 5. It is found that the variation of maximum lateral load is only 3% between the experimental (Test No. 5 of Gomez et al. [12]) and numerical results. Also, it is evident from Figure 5 that the hysteresis loop for the developed FE model and experimental results are quite similar except for the slipping behavior which is due to the complexity of the interactions among the various CBP connection elements. All these validation results suggest that the adopted modeling techniques can be applied with a high degree of confidence for further investigation.

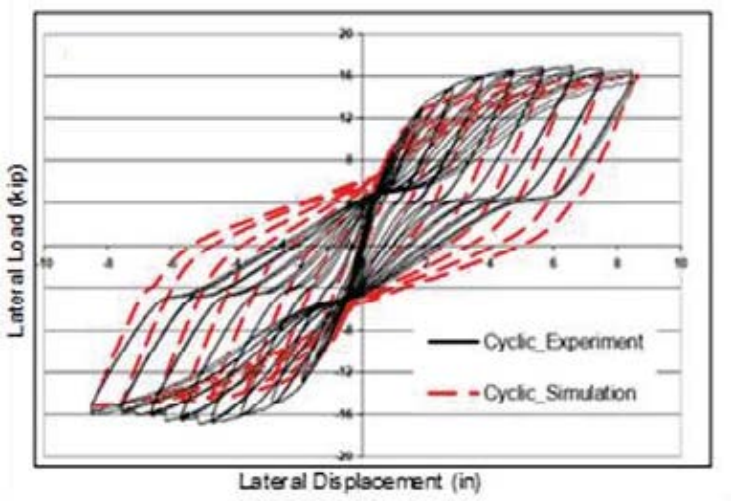

Figure 5: Validation of FE model using cyclic loading

3 PARAMETRIC STUDY

Once validated, a total of 12 FE models are developed for the parametric study to understand the behavioral insights of the CBP connections under combined axial load and biaxial bending. These models consider different practical values for three critical column base connection parameters such as base plate thickness, base plate yield strength and anchor rod diameter. Since no symmetric plane is available when the specimen is subjected to biaxial bending, a full model is considered to simulate the behavior of the CBP connection. Details of the test matrix and development of the bidirectional loading protocol are described in the subsequent sections.

3.1 Parametric analysis cases

The three critical parameters of the analytical investigation are selected from the literature review conducted by Grauvilardell et al. [1] as well as the previous parametric study done by Trautner and Hutchinson [20] where they categorized different parameters of CBP connection into low, medium, and high category. Based on these studies, three critical parameters with variable ranges are considered in this study. Table 4 provides the details of the simulation matrix considered in this parametric study where the bold numbers indicate the variable values of different parameters. Each of the cases considered only one variable to understand its effect on the base plate connection considering PR-01 as the base model.

Parameter	Specimen ID	Parameter Values						
		Base Plate Thickness (mm)	Base Plate Yield Strength (Mpa)	Anchor Rod Dia (mm)	No. of Anchor Rod	Embedment Length (mm)	Grout Thickness (mm)	Axial Load Ratio
Base Model	PR-01	**25**	**350**	**20**	**4**	**500**	**25**	**0.2**
Base Plate Thickness	PR-02	**16**	350	20	4	500	25	0.2
	PR-03	**20**	350	20	4	500	25	0.2
	PR-04	**30**	350	20	4	500	25	0.2
	PR-05	**38**	350	20	4	500	25	0.2

	PR-06	**50**	350	20	4	500	25	0.2
Base Plate Yield Strength	PR-07	25	**300**	20	4	500	25	0.2
	PR-08	25	**400**	20	4	500	25	0.2
Anchor Rod Dia	PR-09	25	350	**16**	4	500	25	0.2
	PR-10	25	350	**25**	4	500	25	0.2
	PR-11	25	350	**30**	4	500	25	0.2
	PR-12	25	350	**38**	4	500	25	0.2

Table 4: Simulation matrix of the parametric study

3.2 General features of the FE models

All the developed FE models of the parametric analysis cases have similar geometric and material properties. ASTM A992 Grade 50 W250x73 column section (typical interior first story column) having 2000 mm length (2/3rd of typical first story height of SMRFs) is designed according to the requirements of CSA S16-19 [21]. The column is designed considering yield strength *(F_y)* of 345 MPa and modulus of elasticity *(E)* of 200 GPa and the cross-section is selected to prevent local buckling criteria as well as its capacity to ensure its effectiveness before the failure of the base plate connection. A rectangular base plate of 407 mm x 407 mm, welded together with the column, having different thicknesses and yield strength is selected for the study. Anchor rods of different sizes are designed using yield strength and modulus of elasticity of 790 MPa and 200 GPa, respectively following the requirements of CSA S16-19 [21] and CSA A23.3-19 [22] to prevent any type of failure in the concrete by pullout or breakout strength. The nut and washers are selected according to standard geometry for the specific anchor rod. A concrete foundation of 1220 mm x1220 mm is designed to support all types of loading. Non-shrink grout having 64 MPa compressive strength of various thickness is also considered between the pedestal and the base plate. All the FE models developed for the parametric analysis study have the same configuration of mesh size, geometric imperfection, tie contact, and interaction properties as the validated full FE model. Anchor rods, nuts and washers and concrete material properties of the developed FE models are also the same as the validated model.

3.3 Bidirectional lateral loading protocol

A bidirectional symmetric lateral loading protocol is developed for the numerical investigation in pursuance of evaluating the effect of biaxial bending on the exposed CBP connection. This cyclic loading protocol is developed for a four-story steel frame building following the concepts discussed in Krawinkler [23] and Elkady [17]. The loading protocol covers a wide range of story drift ratios starting from 0.375% amplitude up to amplitude of 4% radians in the column's strong axis direction as shown in Figure 6(a). It also covers story drift ratio ranging from 0.25% to 2% amplitude in the column's weak axis direction as shown in Figure 6(b). When combined, it is found that the developed bidirectional loading protocol achieves a maximum drift ratio of 3% in the column's strong axis direction when 2% drift amplitude is reached in the column's weak axis direction as depicted in Figure 6(c). Detail procedure of the developed bidirectional loading protocol is described in Elkady [17].

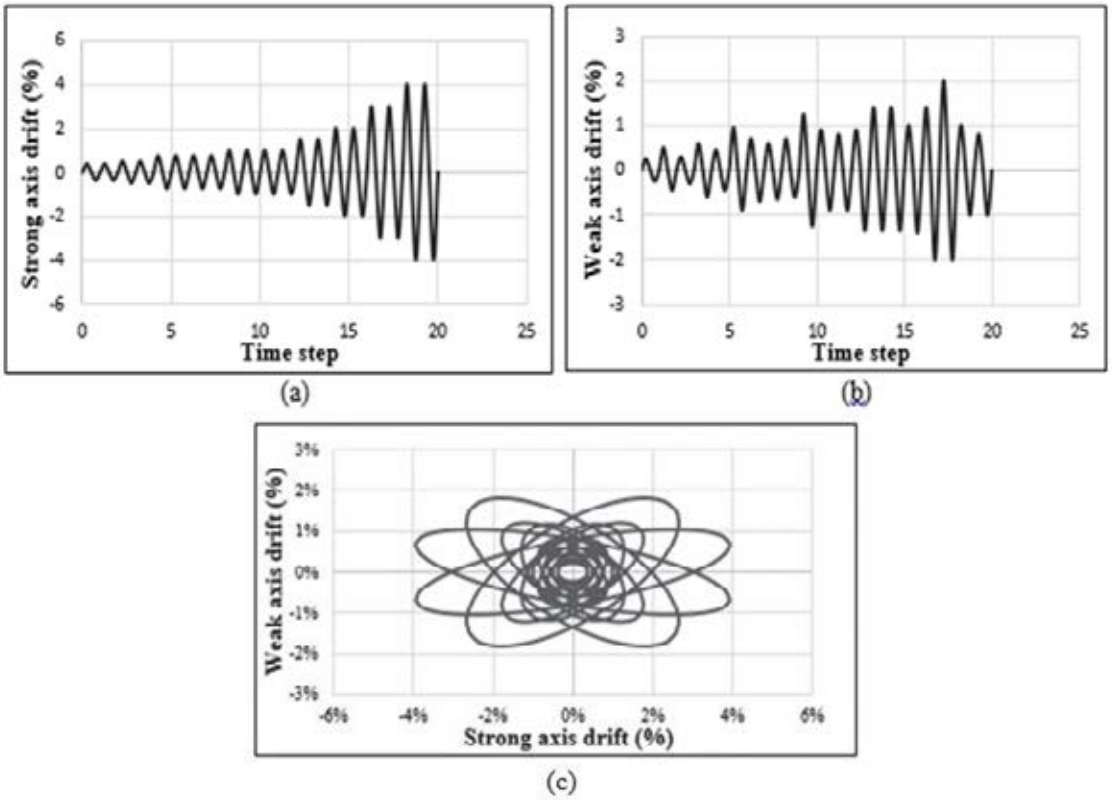

Figure 6: Developed bidirectional symmetric lateral loading protocol: (a) history of strong axis drift ratio; (b) history of weak axis drift ratio; (c) history of strong axis vs weak axis drift ratio

4 RESULTS AND DISCUSSION

The analytical results obtained from the parametric study have been used to further understand the behavior of exposed CBP connections subjected to combined axial load and biaxial bending. Results are scrutinized in terms of moment-rotation curve which is a key output to better understand the connection behavior by defining the rigidity, resistance, and rotational capacity of any connection. Table 5 provides the summary of the results extracted from the FE models.

FE Model ID	Axis	Yield			Ultimate			$K_{\theta(Yield)}$ / $K_{\theta(Ultimate)}$
		M (KN-m)	$\theta \times 10^{-3}$ (rad)	$K_\theta \times 10^3$	M (KN-m)	$\theta \times 10^{-3}$ (rad)	$K_\theta \times 10^3$	
PR-01	X	120.26	13.89	8.66	184.75	33.87	5.45	1.59
	Y	43.28	6.45	6.71	72.20	15.52	4.65	1.44
PR-02	X	49.58	6.68	7.42	78.10	37.38	2.09	3.55
	Y	24.14	3.64	6.63	40.67	16.89	2.41	2.75
PR-03	X	93.22	10.68	8.72	163.81	34.49	4.75	1.84
	Y	40.5	6.57	6.17	63.54	16.07	3.95	1.56
PR-04	X	150.44	12.69	11.85	220.00	32.43	6.78	1.75
	Y	48.68	6.31	7.71	79.43	15.56	5.10	1.51
PR-05	X	155.60	12.65	12.30	244.29	31.40	7.78	1.58
	Y	51.44	6.34	8.11	85.65	15.42	5.55	1.46

PR-06	X	181.52	11.73	15.47	241.43	31.62	7.64	2.03
	Y	53.36	6.27	8.51	89.00	15.25	5.84	1.46
PR-07	X	149.38	21.59	6.92	182.86	33.63	5.44	1.27
	Y	44.52	6.46	6.89	71.91	15.92	4.52	1.52
PR-08	X	154.74	21.67	7.14	195.71	33.09	5.91	1.21
	Y	46.64	6.72	6.94	74.50	15.72	4.74	1.46
PR-09	X	117.20	13.96	8.39	175.71	33.74	5.21	1.61
	Y	37.96	5.19	7.32	71.77	15.81	4.54	1.61
PR-10	X	133.56	13.53	9.87	197.14	33.17	5.94	1.66
	Y	44.98	6.23	7.22	74.64	15.65	4.77	1.51
PR-11	X	132.88	13.48	9.86	205.71	32.89	6.25	1.58
	Y	47.24	6.38	7.41	75.60	15.68	4.82	1.54
PR-12	X	139.34	13.19	10.57	220.00	32.31	6.81	1.55
	Y	46.98	6.42	7.32	76.56	15.59	4.91	1.49

Table 5: Summary of FE model results

4.1 Moment-rotation behavior

For each FE simulation, the hysteretic response in terms of base moment-rotation is plotted as shown in Figure 7 and compared within the various values of the specific parameter considered in the analytical study. Further bilinear moment-rotation curve, considering yield point and ultimate point, is developed for both the strong (x-axis) and weak axis (y-axis) and analyzed separately for convenient visualization. Column plastic moment capacity *(M_p)* is also shown in the same plot (horizontal line) for both strong and weak axis direction. The column base moment *(M)* and base rotation *(θ)* are computed from the column lateral force and lateral displacement according to Eq. (1) and Eq. (2), respectively.

$$M = F \, x \, H_{col} \tag{1}$$

$$\theta = (\Delta_{top} - \frac{F \, x \, H_{col}^3}{3 \, x \, E_{col} \, x \, I_{col}}) \, x \, \frac{1}{H_{col}} \tag{2}$$

Where, F is the lateral force at the column top, H_{col} is the column height from the base plate, Δ_{top} is the displacement at the top of the column, E_{col} is the modulus of elasticity of the column, I_{col} is the column's second moment of inertia in the direction of loading.

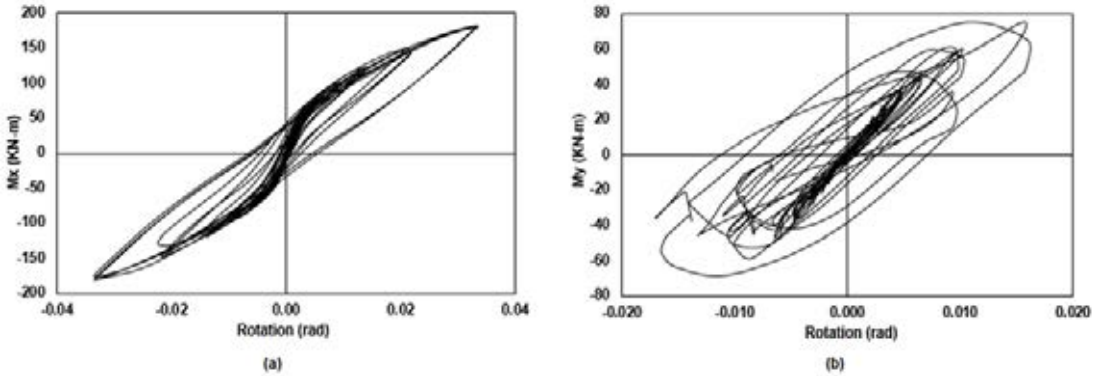

Figure 7: Moment-rotation hysteresis curve for PR-01 model (a) Strong axis (b) Weak axis

4.2 Effect of base plate thickness

Six different base plate thicknesses (PR-01 to PR-06) are considered with values ranging from 16 mm to 50 mm. For the base model (PR-01), the base plate thickness of 25 mm is considered for the study which is widely used in the construction industry. Figure 8 illustrates the comparison of bilinear moment-rotation curves for various base plate thicknesses. It is observed from Figure 8 that a higher value of base plate thickness increases both the stiffness and the strength of the connection for both strong and weak axis direction. This is plausible since an increase in base plate thickness increases the flexural rigidity as well as bending resistance of the plate. However, it should be noted that the effect of base plate thickness is more pronounced in the strong axis direction compared to the weak axis. A significant increase in the strength of the connection is observed after yielding for each of the simulation cases except for the PR-02 where the base plate thickness is considered as 16 mm. Early yielding of the base plate of lower thickness significantly hinders the strength gain of the CBP connection. As reported in Table 5, the average ratio of yield to ultimate rotational stiffness for various base plate thicknesses is 2.06 and 1.7 in the strong and weak axis direction, respectively. It is also found that the strength of all the base connections with different base plate thicknesses is significantly below the column plastic moment capacity in both the strong and weak axis directions. In brief, as the base plate thickness increases, the strength of the base connection is augmented with the reduction in ductility.

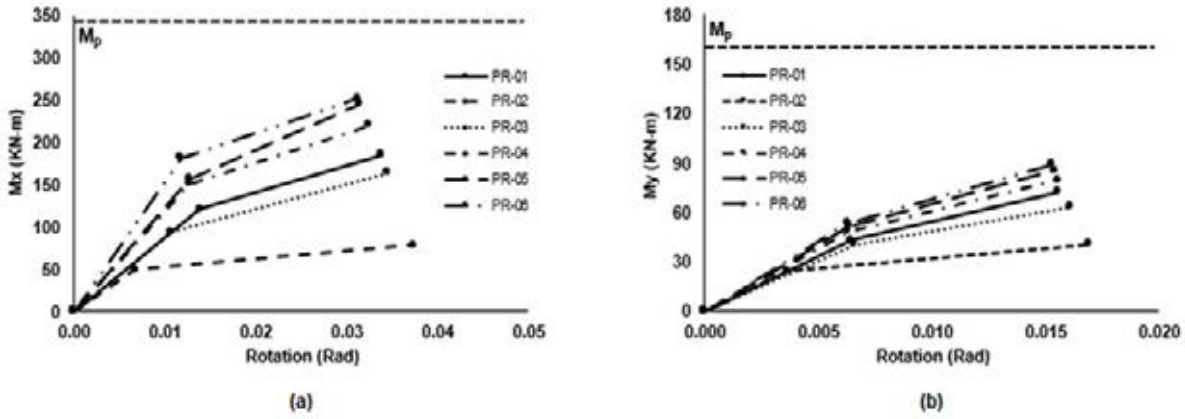

Figure 8: Effect of base plate thickness (a) Strong axis (b) Weak axis

4.3 Effect of base plate yield strength

Different base plate yield strengths of 300, 350 and 400 MPa (PR-01, PR-07 and PR-08) are considered to understand the effect of base plate yield strength on base plate connection behavior. Although base plate yield strength is not considered in the previous experimental study on CBP connections, it is considered in this study due to its contribution on the design of base plate thickness according to AISC Design Guide 1 [8]. The variations in the base plate strengths are considered based on the most commonly used steel grades in industry. It can be seen from Figure 9 and Table 5 that base plate yield strength does not influence the moment-rotation response in the weak axis direction. However, initial stiffness is found to be lower when the base plate yield strength is changed from the base model of 350 MPa in the strong axis direction.

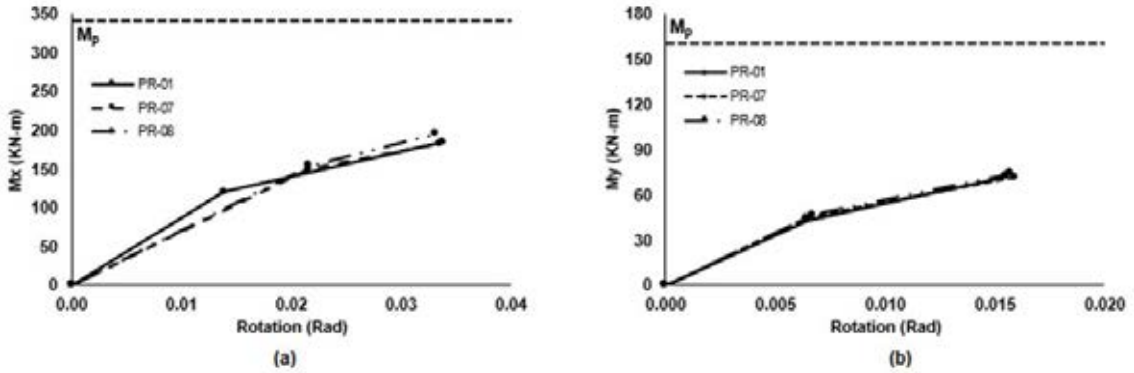

Figure 9: Effect of base plate yield strength (a) Strong axis (b) Weak axis

4.4 Effect of anchor rod diameter

Different anchor bolt diameters ranging from 16 mm to 38 mm (PR-01, PR-09 to PR-12) are selected to scrutinize the moment-rotation behavior of CBP connections. Figure 10 represents the effect of anchor bolt diameter in terms of moment-rotation curves of the base plate connection. It is evident that an increase in anchor bolt diameter increases the initial stiffness as well as the strength in both axes directions. A larger bolt diameter affects the flexibility of the base plate cantilever length by contributing in the base rotation. An increase of 20% is observed for maximum strength in the strong axis direction when the diameter is increased from 20 mm to 38 mm. Conversely, a 6% increment is observed in the weak axis direction for the same configuration. Changes in the initial stiffness are found to be more obvious in the strong axis than the weak axis of the base plate connection. As reported in Table 5, the average ratio of yield to ultimate rotational stiffness is 1.60 and 1.52 in the strong and weak axis direction, respectively.

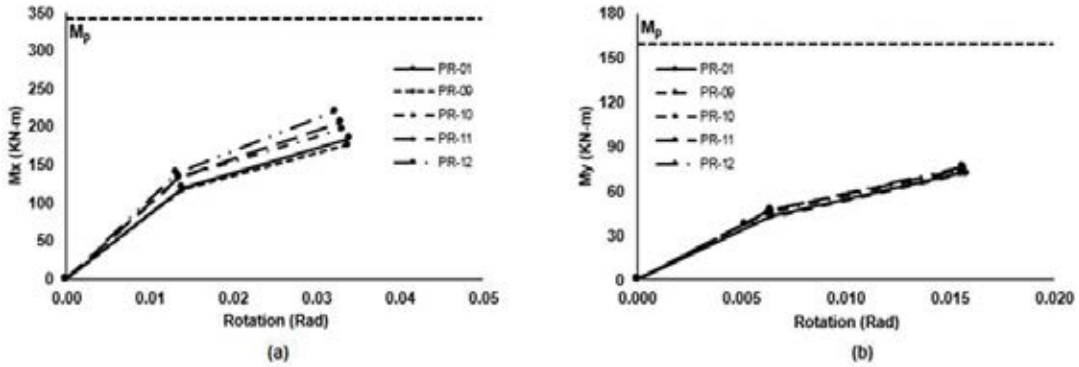

Figure 10: Effect of anchor rod diameter (a) Strong axis (b) Weak axis

5 CONCLUSIONS

- Higher value of base plate thickness increases both the stiffness and the strength of the connection for both strong and weak axis directions.
- The effect of base plate thickness is more pronounced in the strong axis direction compared to the weak axis direction.
- Early yielding of the base plate is observed for the thinner (16 mm) base plate of the CBP connection.
- Base plate yield strength has no significant influence on CBP connection within the considered ranges.

- An increase in anchor bolt diameter increases both the initial stiffness and strength in strong and weak axis directions.
- For different anchor rod diameters, changes in the initial stiffness are found to be more obvious in the strong axis than the weak axis of the base plate connection.

ACKNOWLEDGEMENTS

The financial contributions of the Canadian Institute for Steel Construction (CISC) through CISC Research Grant is gratefully acknowledged.

REFERENCES

[1] J.E. Grauvilardell, D. Lee, J.F. Hajjar, R.J. Dexter, Synthesis of design, testing and analysis research on steel column base plate connections in high seismic zones. *Structural Engineering Rep. No. T-04-02, Dept. of Civil Engineering, University of Minnesota,* Minneapolis, USA, 2005.

[2] R. Tremblay, A. Filiatrault, P. Timler, M. Bruneau, Performance of steel structures during the 1994 Northridge earthquake. *Canadian Journal of Civil Engineering,* **22**(2), 338–360, 1995.

[3] M. Midorikawa, I. Nishiyama, M. Tada, T. Terada, Earthquake and tsunami damage on steel buildings caused by the 2011 Tohoku japan earthquake. *International Symposium on Engineering Lessons Learned from the 2011 Great East Japan Earthquake,* March. Tokyo, Japan, 2012.

[4] J. T. DeWolf, E.F. Sarisley, Column base plates with axial loads and moments. *ASCE Journal of Structural Division,* **106**(11), 2167–2184, 1980.

[5] A. Picard, D. Beaulieu, B. Perusse, Rotational Restraint of a Simple Column Base Connection. *Canadian Journal of Civil Engineering,* **14**, 49-57, 1987.

[6] A. Astaneh-Asl, G. Bergsma, Cyclic Behavior and Seismic Design of Steel Base Plates. *Proceedings of Structures Congress, ASCE,* 409–414, 1993.

[7] J.J. Burda, A.M. Itani, Studies of Seismic Behavior of Steel Base Plates. *Report No. CCEER 99-7, Reno (NV): Center of Civil Engineering Earthquake Research, Department of Civil and Environmental Engineering,* University of Nevada, NV, USA, 1999.

[8] J.M. Fisher, L.A. Kloiber, *Design Guide 1: Base plate and anchor rod design, 2nd Ed.* American Institute of Steel Construction, Chicago, 2006.

[9] M. Fahmy, B. Stojadinovic, S.C. Goel, Analytical and experimental behavior of steel column bases. *Proceedings of 8th Canadian Conference on Earthquake Engineering, Canadian Association for Earthquake Engineering,* Ottawa, ON, Canada, 1999.

[10] D.Y. Lee, S.C. Goel, B. Stojadinovic, Exposed Column-Base Plate Connections Bending about Weak Axis: I. Numerical Parametric Study. *International Journal of Steel Structure,* KSSC, **8**(1), 11–27, 2008.

[11] D.Y. Lee, S.C. Goel, B. Stojadinovic, Exposed column-base plate connections bending about weak axis: II. Experimental Study. *International Journal of Steel Structure,* KSSC, **8**(1), 29–41, 2008.

[12] I. Gomez, G. Deierlein, A. Kanvinde, Exposed column base connections subjected to axial compression and flexure. *Final Rep. Presented to the American Institute of Steel Construction,* Chicago, USA, 2010.

[13] A.M. Kanvinde, S.J. Jordan, R.J. Cooke, Exposed column baseplate connections in moment frames—Simulations and behavioral insights. *Journal of Constructional Steel Research,* **84**, 82–93, 2013.

[14] M.A.K. Fasaee, M.R. Banan, S. Ghazizadeh, Capacity of Exposed Column Base Connections Subjected to Uniaxial and Biaxial Bending Moments. *Journal of Constructional Steel Research,* **148**, 368–370, 2018.

[15] B. Song, C. Galasso, A. Kanvinde, Reliability Analysis and Design Considerations for Exposed Column Base Plate Connections Subjected to Flexure and Axial Compression. *ASCE Journal of Structural Engineering,* **147**(2), 04020328, 2021.

[16] SIMULIA Inc. *ABAQUS user's manual, version 6.20. Providence,* RI, USA, 2020.

[17] A. Elkady, Collapse Risk Assessment of Steel Moment Resisting Frames Designed with Deep Wide Flange Columns in Seismic Regions. *PhD Thesis, Department of Civil Engineering and Applied Mechanics,* McGill University, Montreal, Canada, 2016.

[18] I.S, Grigoriev, E.Z. Meĭlikhov, A.A. Radzig, *Handbook of Physical Quantities*. CRC Press, Boca Raton, FL, 1997.

[19] J.L. Chaboche, A review of some plasticity and viscoplasticity constitutive theories. *International Journal of Plasticity,* **24**(10), 1642–1693, 2008.

[20] C.A. Trautner, T.C. Hutchinson, Parametric Finite-Element Modeling for Exposed Steel Moment Frame Column Baseplate Connections Subjected to Lateral Loads. *ASCE Journal of Structural Engineering,* **144**(6), 04018049, 2018.

[21] CSA. *Design of Steel Structures. CSA-S16-19, Canadian Standards Association,* Toronto, ON, Canada, 2019.

[22] CSA. *Design of Concrete Structures. CSA-A23.3, Canadian Standards Association,* Mississauga, ON, Canada, 2019.

[23] H. Krawinkler, Cyclic loading histories for seismic experimentation on structural components. *Earthquake Spectra,* **12**(1), 1–12, 1996.